

FORCE INTERACTION OF ARC CURRENT WITH SELF-MAGNETIC FIELD*

V.F. DEMCHENKO¹, I.V. KRIVTSUN¹, I.V. KRIKENT² and I.V. SHUBA¹

¹E.O. Paton Electric Welding Institute, NASU

11 Kazimir Malevich Str., 03680, Kiev, Ukraine. E-mail: office@paton.kiev.ua

²Dneprosky State Technical University

2 Dneprostrojevskaya Str., 51918, Kamenskoe, Ukraine

Detailed theoretical analysis of force interaction of welding current with self-magnetic field under the conditions of nonconsumable electrode arc welding was performed. Electromagnetic force (Lorentz force) is presented as a sum of vortex and potential forces, from which only the vortex component is capable of exciting the movement of plasma or molten metal. Centripetal vortex force generates magnetic pressure in arc plasma and weld pool metal. The gradient of this pressure induces magnetic force, oriented predominantly in the axial direction. The magnitude of this force is the greater the higher the current density in near-anode region of welding arc (on weld pool surface). Depending on the nature of electric current spreading in the arc column, three possible scenarios of arc plasma movement are considered: by the schematic of right and inverse cone, as well as in the form of two vortices, excited by current channel compression in near-cathode and near-anode regions of the arc. Presented theoretical postulates are illustrated by numerical calculations of distribution of magnetic pressure and magnetic forces in arc column plasma and in weld pool metal. It is established that electric current contraction on the anode intensifies hydrodynamic flows of molten metal, and, therefore, also convective energy transfer from central zone of weld pool surface to its bottom part, promoting an increase of penetrability of the arc with refractory cathode. 14 Ref., 1 Table, 12 Figures.

Keywords: arc welding, nonconsumable electrode, molten metal, hydrodynamic flows, arc current, magnetic field, arc penetrability

In arc welding, electromagnetic force, arising as a result of interaction of arc current with self-magnetic field, has an essential influence on the processes of transfer of mass, pulse and energy, both in welding arc column, and in weld pool. In arc plasma Lorentz force is the dominating force factor, determining the structure and intensity of plasma flows. In principle, the nature of gas-dynamic flow of plasma in arc column can vary, depending on its length and transverse dimensions of the regions of arc cathode and anode attachment, which determine the magnitude of ponderomotive force in near-electrode zones of arc column, and, accordingly, structure of gas-dynamic flows of arc plasma as a whole. In the weld pool, alongside electromagnetic force, three more forces are applied to the melt, namely Marangoni thermocapillary force, due to temperature dependence of surface tension factor, and force of viscous friction of arc plasma flow against molten metal surface, acting along weld pool free surface, as well as buoyancy (Archimedean) force, arising due to nonuniformity of the melt temperature field. The latter is the least significant factor

in formation of molten metal flows, compared to Lorentz force, Marangoni force and friction force. Dominating role of one of these three force factors depends on welding mode, properties of metal being welded, weld pool dimensions, size of arc attachment region on pool surface, and other welding process characteristics.

As is known, bulk density of electromagnetic force \vec{F} is found from the following formula $\vec{F} = \vec{j} \times \vec{B}$, where \vec{j} is the vector of electric current density; \vec{B} is the vector of magnetic induction. In such a form, electromagnetic force is taken into account in numerous studies (see, for instance, [1–8]), devoted to simulation of the processes of mass, pulse and energy transfer in the arc discharge and in weld pool metal. The given formula for calculation of electromagnetic force allows quite adequate determination of welding current influence on plasma movement in arc column and weld pool hydrodynamics. At the same time, vector field of electromagnetic forces, determined by this formula, does not allow a priori estimation on qualitative level of possible structure of these gas(hydro)

*Based on a report presented at the VIII International Conference «Mathematical Modelling and Information Technologies in Welding and Related Processes», September 19–23, 2016, Odessa, Ukraine.

dynamic flows. The latter can be revealed only a posteriori, after performance of respective calculations of the characteristics of plasma and molten metal flows, initiated by electromagnetic force. This drawback of standard expression for bulk density of electromagnetic force, is due to the fact that this force, similar to bulk force of any other physical nature, is represented as a sum of potential and vortex components, from which only the vortex component of the force is capable of exciting the movement of the medium. Therefore, it is of interest to isolate the vortex component from total electromagnetic force \vec{F} , and on this basis to uncover the mechanism and features of action of this important component of the force on arc column plasma and weld pool molten metal. This is exactly the standpoint from which detailed theoretical analysis of force interaction of welding current with self-magnetic field is performed in this paper. This analysis is confirmed by specific calculations of spatial distributions of electromagnetic field characteristics (electric current density, magnetic field intensity, bulk density of vortex component of Lorentz force, magnetostatic pressure) in arc plasma column and in weld pool metal, made for characteristic conditions of nonconsumable electrode welding.

Main theoretical postulates. In arc plasma and in molten metal, magnetic induction vector \vec{B} is connected with magnetic field intensity vector \vec{H} by relationship $\vec{B} = \mu_0 \mu \vec{H}$ where μ_0 is the universal magnetic constant; μ is the magnetic permeability of conducting medium. Then, the formula for bulk density of electromagnetic force can be rewritten as

$$\vec{F} = \mu_0 \mu (\vec{j} \times \vec{H}). \quad (1)$$

In the stationary case the following relationship is in place that relates self-magnetic field intensity \vec{H} with electric current density \vec{j}

$$\text{rot } \vec{H} = \vec{j}. \quad (2)$$

At relatively low speeds of arc movement characteristic for nonconsumable electrode welding, electromagnetic field in arc plasma can be taken to be axisymmetric with good approximation. Such a nature of distribution of field characteristics is preserved also in the volume of metal being welded near the region of anode attachment of the arc. In the cylindrical system of coordinates (r, θ, z) for axisymmetric electromagnetic field we have $\vec{j} = \{j_r, 0, j_z\}$, $\vec{H} = \{0, H_\theta, 0\}$

It follows from equation (2) that

$$-\frac{\partial H_\theta}{\partial z} = j_r; \quad \frac{1}{r} \frac{\partial (r H_\theta)}{\partial r} = j_z$$

then

$$\vec{F} = -\mu_0 \mu \left[H_\theta \frac{1}{r} \frac{\partial}{\partial r} (r H_\theta) \vec{e}_r + H_\theta \frac{\partial H_\theta}{\partial z} \vec{e}_z \right],$$

where $\{\vec{e}_r, \vec{e}_z\}$ are the unit vectors in the direction of the respective coordinate axes. We will transform the resulting expression to the following form

$$\vec{F} = -\mu_0 \mu \left(\frac{1}{2} \text{grad } H_\theta^2 + \frac{H_\theta^2}{r} \vec{e}_r \right). \quad (3)$$

By Helmholtz theorem, any vector field can be represented in the form of a sum of two vector fields \vec{F}_{pot} and \vec{F}_{rot} , the first of which is the potential and the second one is the vortex field. In keeping with (3), potential and vortex components of Lorentz force are expressed as follows in terms of the square of azimuthal component of magnetic field intensity:

$$\vec{F}_{pot} = -\mu_0 \mu \frac{1}{2} \text{grad } H_\theta^2, \quad \vec{F}_{rot} = -\mu_0 \mu \frac{H_\theta^2}{r} \vec{e}_r. \quad (4)$$

Let us consider the equation of movement of viscous incompressible liquid in the field of electromagnetic force \vec{F}

$$\rho \frac{D\vec{V}}{Dt} = -\text{grad } P + \eta \Delta \vec{V} + \vec{F}, \quad (5)$$

where ρ is the density; \vec{V} is the vector of medium movement velocity; $D\vec{V}/Dt$ is the substantial derivative; P is the hydrodynamic pressure; η is the dynamic viscosity coefficient. Taking (4) into account, in the case of axisymmetric electromagnetic field, equation (5) can be written in the following form

$$\rho \frac{D\vec{V}}{Dt} = -\text{grad } P' + \eta \Delta \vec{V} + \vec{F}_{rot}. \quad (6)$$

Here $P' = P + P_{ms}$, where $P_{ms} = 0,5 \mu_0 \mu H_\theta^2$ is the magnetostatic pressure. A similar representation for pressure also holds for equations of magnetic gas dynamics of arc plasma. It follows from (6) that in an axisymmetric electromagnetic field the movement of liquid (plasma) proceeds solely as a result of action of centripetal vortex component of force

$\vec{F}_{rot} = -\frac{H_\theta^2}{r} \vec{e}_r$. Now, the action of potential force \vec{F}_{pot} is limited to creation of magnetostatic pressure P in moving substance volume, compensating the potential component of the force, and not preventing the medium movement under the impact of mass force of another physical nature, for instance, the buoyancy force. Note, that magnetostatic pressure is distributed in a complex manner through the volume of electrically conducting medium.

By the theorem of total current, magnetic field intensity $H_\theta(r, z)$ can be represented in the following

form $H_\theta(r, z) = \frac{I(r, z)}{2\pi r}$, where $I(r, z) = \int_0^r j_z(r', z) r' dr'$ is the electric current flowing within a circle of radius r , in arbitrary axial section z . Thus, vortex component of Lorentz force $\vec{F}_{rot}(r, z)$ and magnetostatic pressure P_{ms} can be expressed as current $I(r, z)$ in the following form:

$$\begin{aligned} \vec{F}_{rot}(r, z) &= -\mu_0 \mu \frac{I^2(r, z)}{4\pi^2 r^3} \vec{e}_r; \\ P_{ms}(r, z) &= \frac{\mu_0 \mu}{8\pi^2} \frac{I^2(r, z)}{r^2}. \end{aligned} \quad (7)$$

Near the axis of symmetry $I(r, z) = 0(r^2)$, so that $\vec{F}_{rot}(r, z) \rightarrow 0, P_{mag}(r, z) \rightarrow 0$ at $r \rightarrow 0$. Formulas (7) are similar to those used at description of pinch-effect. At relatively small welding currents (of the order of 100–200 A) arc discharge compression (pinch-effect) is weak, and the action of centripetal force \vec{F}_{rot} is realized by excitation of axial flow of arc plasma or weld pool metal. For qualitative analysis of the mechanism of action of force $\vec{F}_{rot}(r, z)$ on gas(hydro)dynamic flows, let us turn to equations of magnetic hydrostatics. Neglecting inertia and viscosity forces in (5), we will have

$$-\text{grad} P' + \vec{F} = 0. \quad (8)$$

In terms of pressure $P'(r, z)$ the system of equations (8), taking into account (3), is written as

$$\begin{cases} \frac{\partial P'}{\partial r} = -\mu_0 \mu \frac{H_\theta^2}{r}; \\ \frac{\partial P'}{\partial z} = 0. \end{cases} \quad (9)$$

In the context of magnetostatics equations (9), pressure $P'(r, z)$ created by vortex component of Lorentz force, can be interpreted as magnetic pressure, so that further on we will denote it as $P_{mag}(r, z) = P'(r, z)$. Let us integrate the first of equations (9) in the range of $[r, \infty)$, assuming that $P'(r, z)$ vanishes at $r \rightarrow \infty$ (due to the fact that $\lim_{r \rightarrow \infty} H(r, z) = 0$). We have the following expression for $\vec{P}_{mag}^\infty(r, z)$

$$P_{mag}(r, z) = P_{mag}^{(0)} - \mu_0 \mu \int_0^r \frac{H_\theta^2(r', z)}{r'} dr', \quad (10)$$

where $P_{mag}^{(0)}(0, z) = \mu_0 \mu \int_0^\infty \frac{H_\theta^2(r', z)}{r'} dr'$ is the magnetic pressure on system axis. Magnetic field gradient creates force $\vec{F}_{mag} = \text{grad} P_{mag}(r, z)$, which is distributed in a complex way in the bulk of electrically conducting

medium. Note that the second of magnetostatics equations (9) is satisfied only when $j_r \equiv 0$ in the current channel. In the general case of axisymmetric Lorentz force, defined by equation (3), the impact of force \vec{F}_{mag} is balanced in equations of magnetic hydrostatics (8) (or equations of magnetic gas(hydro)dynamics) by forces of non-magnetic origin, in which the pressure resulting from dynamic velocity head can have the dominant role.

Force impact of magnetic field of welding current on arc plasma. Intensity and direction of gas-dynamic flows in arc plasma, excited by vortex component of Lorentz force, depend on the ratio of dimensions of current-conducting channels in near-electrode regions of the arc. Let us analyze three characteristic scenarios of plasma flow movement (Figure 1), differing by the nature of electric current spreading in arc column.

Scenario 1. Let us consider straight polarity non-consumable electrode welding. Let R_a be the radius of anode attachment of the arc; R_c is the radius of cathode attachment. At $R_a > R_c$ electric current in arc column spreads by «right» cone schematic, so that vortex component of Lorentz force \vec{F}_{rot} and magnetic pressure P_{mag} reach the greatest values near the cathode (see Figure 1, a), where current density is maximum, and decrease towards the anode. This results in an axial gradient of magnetic pressure in arc column plasma, which causes plasma flow in the axial direction (from cathode to anode) with subsequent formation of bell shape of the arc column.

Scenario 2. In welding over a layer of activating flux (A-TIG process), as a result of arc contraction on the anode, it is anticipated that transverse dimensions of current-conducting channels near the cathode and anode will be commensurate. Then, distribution of vortex component of Lorentz force by column height acquires two maximums, located near the cathode and anode. Magnetic pressure is distributed in a similar

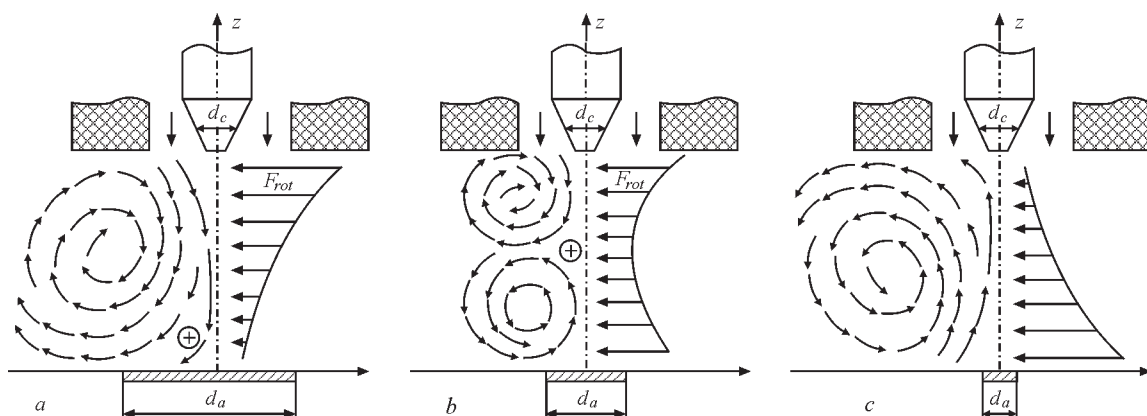


Figure 1. Distribution of vortex component of Lorentz force and plasma flow pattern in welding arc column: a — scenario 1; b — scenario 2; c — scenario 3

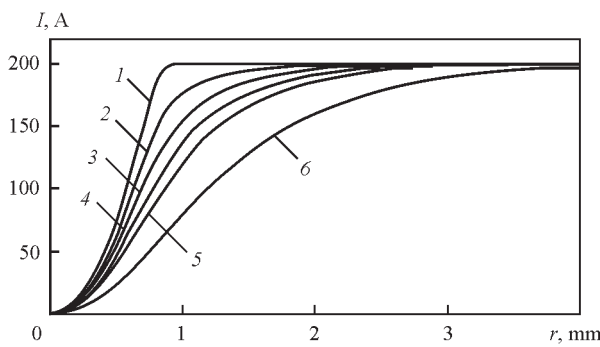


Figure 2. Change of current $I(r)$ in near-cathode region of arc column

fashion. Its gradient causes formation of two opposite vortex flows of plasma in the arc column (see Figure 1, *b*), directed from cathode and anode towards the middle (by height) part of arc column. Their interaction leads to formation of barrel shape of the column. Therefore, gas-dynamic pressure of arc column, as a factor of deformation of weld pool free surface, is in place only under the conditions of scenario 1.

Scenario 3. If $R_c > R_a$, then current spreading proceeds by «inverse cone» schematic. In TIG welding such a scenario is improbable. It, however, can be in place in hybrid laser-arc welding, when plasma flows can be directed towards the cathode (see Figure 1, *c*).

Let us illustrate the features of distribution of vortex component of electromagnetic force and magnetic pressure for free-burning argon arc 3 mm long at current $I = 200$ A (TIG welding). For this purpose we will use the results of numerical simulation [9] of distributed characteristics of arc discharge plasma, performed in keeping with arc model proposed in [10]. During analysis of results, we will prefer near-cathode region of arc column, where the current channel size is the smallest, and, accordingly, the greatest density of electric current is achieved (Figure 2). To illustrate electromagnetic field characteristics in this region, we will single out six cross-sections of arc column, namely: 1 — directly on the column boundary with cathode region; 2–6 — at distances of 0.1; 0.2; 0.3; 0.4; 0.8 mm from this boundary, respectively (in Figures 3–5 the figures on the curves indicate the section

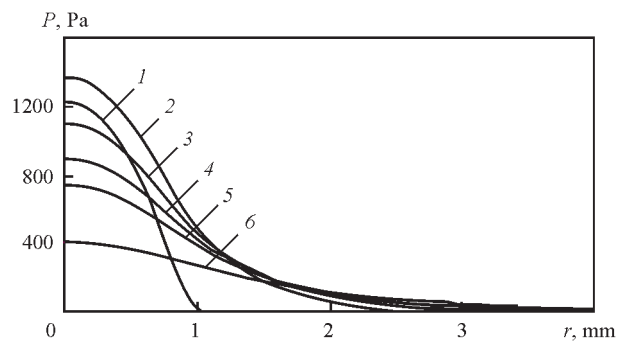


Figure 4. Distribution of magnetic pressure near the cathode number). Nature of variation of current $I(r, z)$ flowing within a circle of radius r (see Figure 2), is indicative of the fact that in the considered case electric current spreading in arc column occurs by the schematic of «right cone» and, therefore, gas-dynamic processes in the arc discharge develop in keeping with scenario 1.

Modulus of vortex component of Lorentz force \vec{F}_{rot} , calculated depending on $I^2(r, z)$ by formula (7), has a maximum (Figure 3) reached in selected arc column sections at $r \approx 1$ mm, this maximum value decreasing rapidly, when moving away from the cathode. The impact of compressive force \vec{F}_{rot} in near-cathode zone of arc column induces magnetic pressure P_{mag} , the maximum value of which is achieved on the arc axis. Magnetic pressure rapidly decreases with increasing distance from the cathode (Figure 4), resulting in formation of high gradient of magnetic pressure $grad P_{mag} = \vec{F}_{mag}$ in near-cathode plasma, which generates force F_{mag} near the cathode, directed predominantly towards the anode. In terms of this calculation of electromagnetic field in arc discharge, axial component \vec{F}_{mag} turns out to be quite significant and is equal to more than $2 \cdot 10^6$ N/m³.

Force \vec{F}_{mag} excites plasma flow in arc column (Figure 5), predominantly directed towards the anode. This flow has an acceleration section at the distance of about 1 mm from the cathode that corresponds to the region of highest values of the modulus of magnetic pressure gradient. Velocity of plasma flow in the cen-

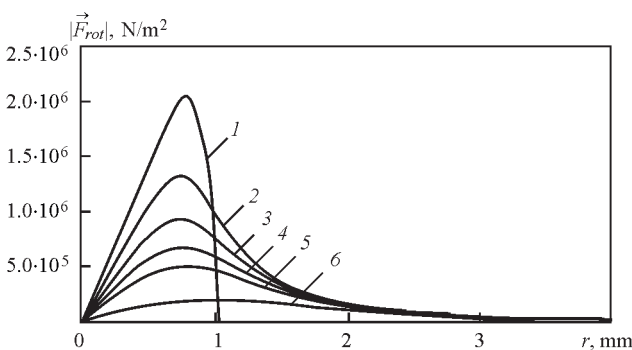


Figure 3. $|\vec{F}_{rot}|$ distribution in cross-sections of near-cathode region of arc column

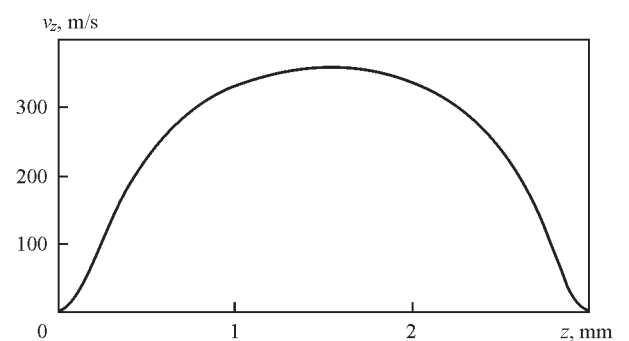


Figure 5. Distribution of velocity of plasma movement along the arc axis (coordinate z is calculated from the cathode region boundary)

tral part of arc axial region is here equal to hundreds of meters per second.

Impact of Lorentz force on weld pool metal. To analyze the force impact of self-magnetic field of arc current on weld pool metal, let us consider the model of charge transfer in the sample being welded (arc anode) of thickness L , in the assumption that electromagnetic field in the metal preserves axial symmetry, inherent to arc plasma. Let $\varphi(r, z)$ be the scalar potential of electric field, and let $\vec{j}(r, z) = -\sigma \text{grad} \varphi$ be the density of electric current in the metal, where σ is its specific electric conductivity. Then, we will have the following equation from the law of conservation of electric charge $\text{div} \vec{j} = 0$.

$$\frac{1}{r} \frac{\partial}{\partial r} \left(r \sigma \frac{\partial \varphi}{\partial r} \right) + \frac{\partial}{\partial z} \left(\sigma \frac{\partial \varphi}{\partial z} \right) = 0. \quad (11)$$

We will integrate equation (11) in the domain of $\Omega = \{0 < r < R, 0 < z < L\}$, where we will select a rather large radius of calculation region R for free spreading of current.

Let us formulate boundary conditions. On sample surface $z = 0$, we will assign the distribution of axial component of electric current density by Gaussian law, i.e. we will assume

$$j_z(r, 0) = j_0 \exp(-a^2 r^2), \quad (12)$$

where j_0 is the axial value of current density. Parameters j_0 and a are found from the following conditions:

$I = 2\pi \int_0^\infty j_z(r, 0) r dr$, $j_z(R_e, 0) = j_0 e^{-2}$, where I is the assigned welding current; $R_e = \frac{\sqrt{2}}{a}$ is the effective radius of current-conducting channel on sample surface (anode).

At $r = 0$ and $r = R$ we will assign the natural boundary conditions as follows:

$$\left. \frac{\partial \varphi}{\partial r} \right|_{r=0} = \left. \frac{\partial \varphi}{\partial r} \right|_{r=R} = 0. \quad (13)$$

On plate lower surface, assuming that the sample being welded is pressed tightly to the copper backing, we will take the potential to be constant and equal to zero

$$\varphi(r, L) = 0. \quad (14)$$

In order to analyze the influence of the size of current-conducting channel in the arc anode region on force interaction of current with self-magnetic field, three effective radii of current-conducting channel were considered: $R_e = 1; 2; 3$ mm. Respective distributions of current density on the anode surface at current $I = 100$ A are given in Figure 6.

As specific electric conductivity of metal greatly exceeds that of plasma, the current coming to the metal from arc anode region, quickly spreads through the metal volume. The pattern of current spreading can be traced by distribution of current lines in the sam-

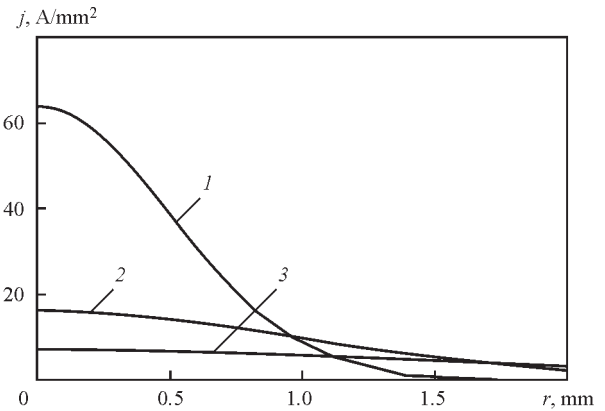


Figure 6. Distribution of current density over the anode surface: 1 — R_e ; 2 — 2; 3 — 3 mm

ple being welded (Figure 7). Here, the current line refers to a line, outlining the volume of metal, through which current of a specified value flows (Figure 7 shows current lines $I = 10; 30; 50; 70$ and 90 A). Similar patterns of current spreading in the metal being welded by «right cone» schematic are in place also at other radii of current channel on anode surface.

Let us analyze the influence of the size of anode current channel on distribution of electromagnetic field characteristics in the metal being welded. Figure 8 gives for $R = 1; 2; 3$ mm, radial distributions of azimuthal component of magnetic field intensity H_θ in different sections across sample thickness. In keeping with the theorem of total current, magnetic field intensity as a function of radius, first rises monotonically, reaches a maximum and then decreases to zero at $r \rightarrow \infty$ as $1/r$. At the change of R_e in the range of 1–3 mm, H_θ maximum on sample surface and in underlying sections decreases rapidly, and its position shifts towards larger radii.

As the vortex component of electromagnetic force is quadratically dependent on magnetic field intensity, the above-mentioned tendency also holds for $|\vec{F}_{rot}(r, z)|$ distribution in the sample volume (Figure 9) with the only difference that $\max |\vec{F}_{rot}|$ decreases by orders of magnitude at increase of the size of effective radius of current-conducting channel on anode surface from 1 to 3 mm.

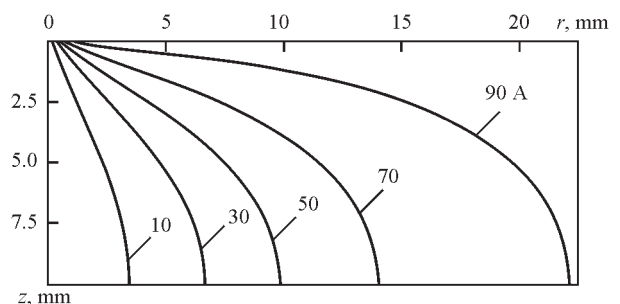


Figure 7. Current spreading in the sample being welded (anode) at $R_e = 1$ mm

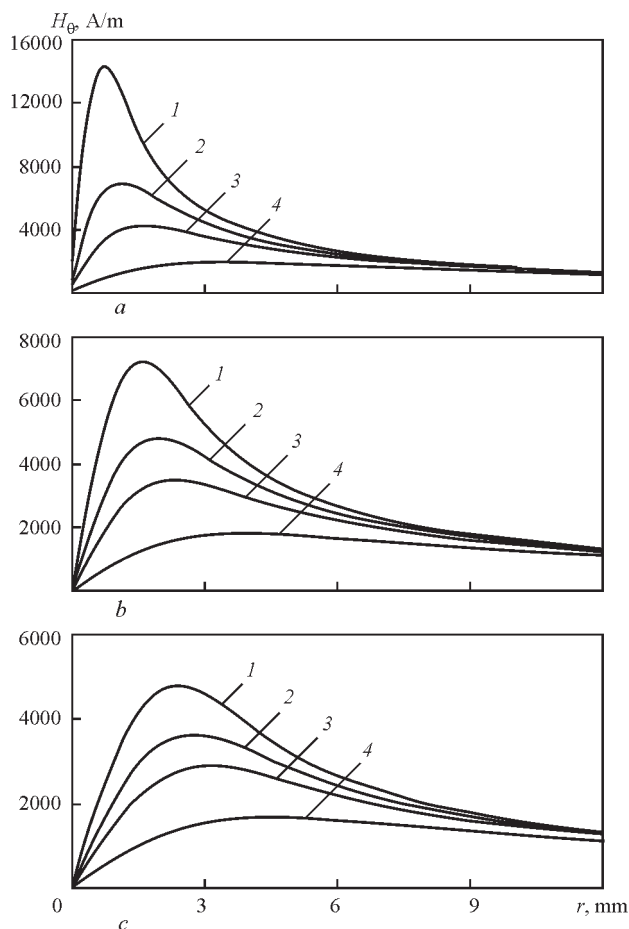


Figure 8. Magnetic field intensity in the sample being welded: *a* — $R_e = 1$; *b* — 2; *c* — 3 mm ($I - z = 0$; 2 — 0.5; 3 — 1; 4 — 2.5 mm)

Before we go over to analysis of magnetic pressure distribution in the metal, due to action of force \vec{F}_{rot} , let us indicate two fundamental differences of force impact of welding current on arc plasma and on metal being welded. The first of them consists in that current flowing in arc plasma is limited by a region, in which electric conductivity of plasma is different from zero (tentatively, this current-conducting channel in the case of Ar corresponds to the region, where plasma temperature is higher than 5000 K), whereas in the metal being welded current flows freely and the current-conducting channel is not limited in any way. Second difference is connected with formation of magnetic pressure in arc plasma. In arc column magnetic pressure on the axis (see (10)) and in arc plasma, as a whole, is determined by the impact of vortex component of electromagnetic force in the range of $0 \leq r < \infty$, while in solid metal \vec{F}_{rot} impact is balanced by the forces of elasticity and does not in any way influence magnetic pressure in the weld pool. Thus, magnetic pressure in the weld pool forms due to force impact of just that part of welding current, which flows through the weld pool, and, therefore, depends on pool shape and dimensions. Taking this feature

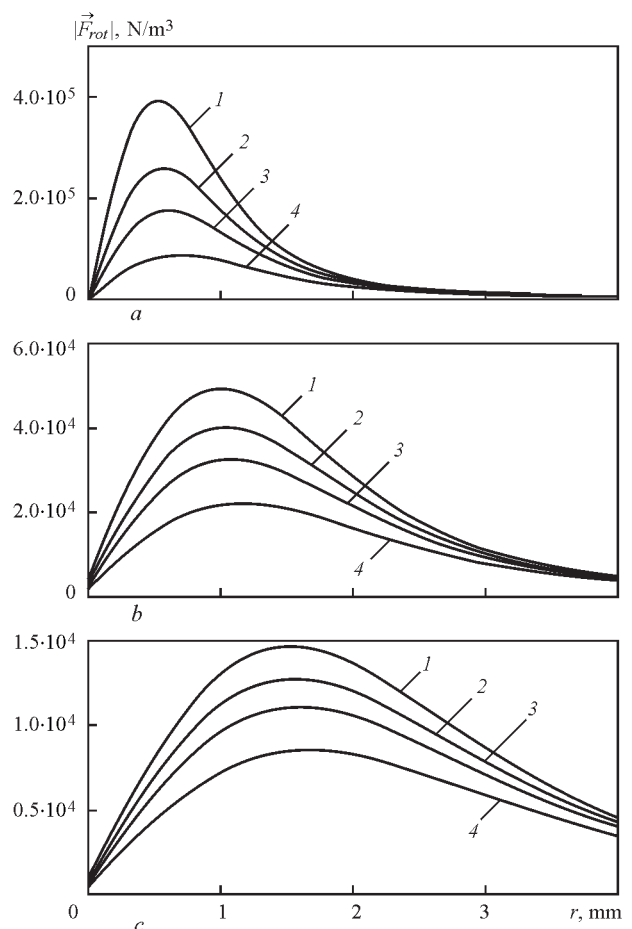


Figure 9. F_{rot} distribution in the sample volume: *a* — $R_e = 1$; *b* — 2; *c* — 3 mm ($I - z = 0$; 2 — 0.5; 3 — 1; 4 — 2.5 mm)

into account, we will transform expression (10) for magnetic pressure in the weld pool. Let $R^* = R^*(z)$ be the expression, describing the pool shape at a certain moment of time. Integrating the first of equations (9) in the interval of $[0, R^*(z)]$, we will obtain the following expression for magnetic pressure distribution in the weld pool

$$P_{mag}(r, z) = \mu_0 \mu \int_r^{R^*} \frac{H^2(r', z)}{r'} dr'. \quad (15)$$

Let us consider this distribution, depending on pool dimensions and effective radius of current channel on anode surface. For qualitative analysis, we will proceed from the assumption that the pool has the shape of a hemisphere of radius R_v . Figure 10 presents the calculated data on magnetic pressure distribution in near-surface region of the pool, depending on effective radius R_e of current-conducting channel at $R = 1; 2$ mm.

As the share of welding current flowing through the weld pool, is increased with increase of its size, magnetic pressure on the pool surface and in its volume is essentially increased with R_v increase for all radii of current-conducting channel on the anode (compare the right and left curves in Figure 10). The

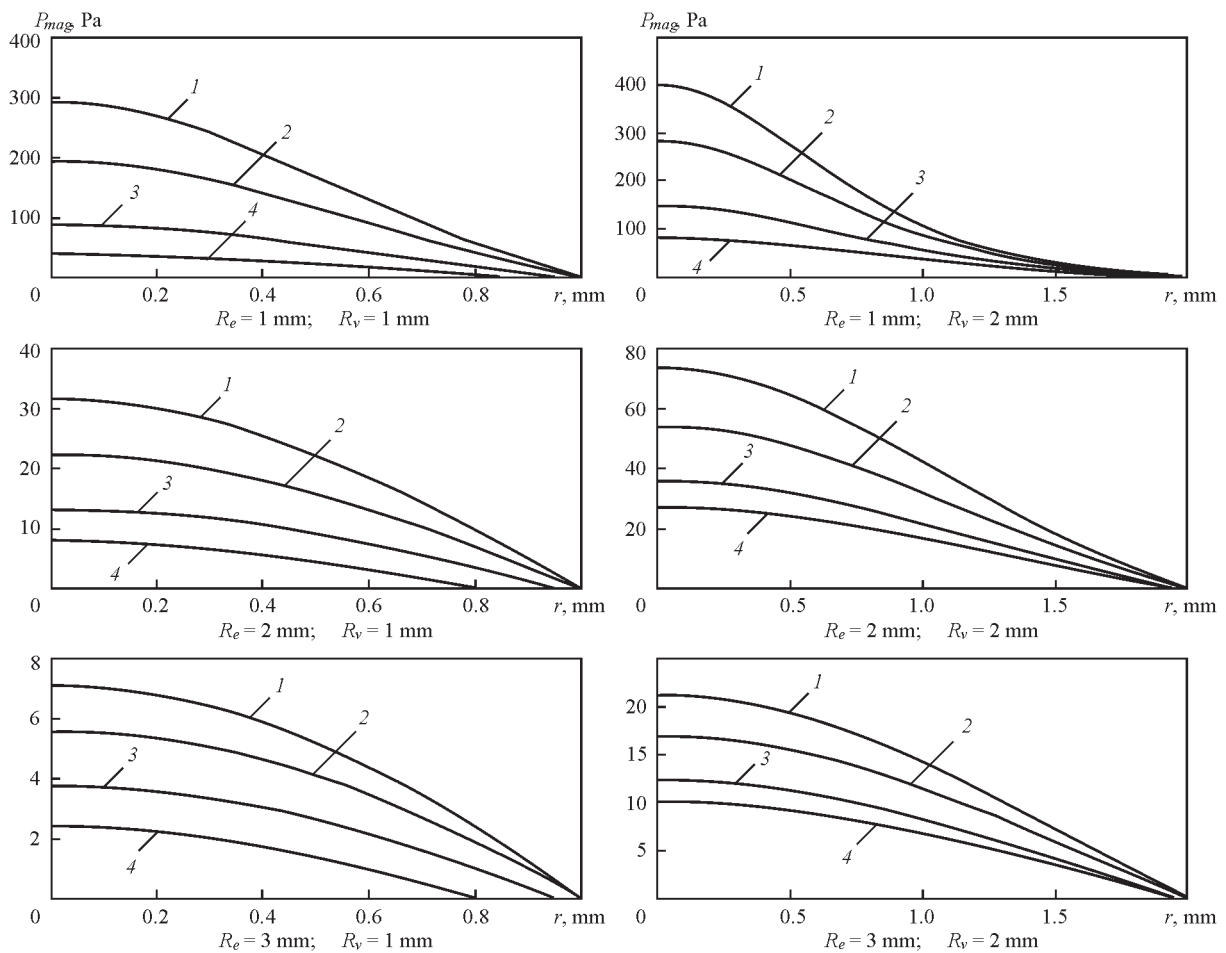


Figure 10. Distribution of magnetic pressure in the weld pool: 1 — $z = 0$; 2 — 0.15; 3 — 0.35; 4 — 0.5 mm

second conclusion which follows from calculated data given in Figure 10, consists in that the magnitude of magnetic pressure in the melt largely depends on the size of current-conducting channel on the anode: with R_e increase, magnetic pressure on the pool surface and in its volume decreases by an order of magnitude. Note that maximum magnetic pressure, reached on the pool surface at $R_e = 1$ mm; $R_v = 2$ mm, is equal to 400 Pa. This value is equal to just 0.4 % of atmospheric pressure and, at first glance it seems that magnetic pressure can be neglected. This, however, is not so, as shown by quantitative estimates derived from Bernoulli theorem for incompressible liquid. In keeping with the latter, $P_{mag} + \frac{\rho V^2}{2} = \text{const}$, i.e. in this case magnetic pressure is balanced by velocity head $\rho V^2/2$, where ρ is the metal density, V is the velocity of melt movement (the latter refers to axial component of velocity vector). For numerical estimate, we will select two sections on pool axis $z = 0$, $z = h$, the first of which corresponds to melt surface, and the second is located in-depth of the melt, where magnetic pressure is small ($P(h) \approx 0$ at $h \approx 1$ mm). We will assume $V(0) = 0$, then $V(h) \approx \sqrt{2P_{mag}^{(0)} / \rho}$, where $P_{mag}^{(0)}$ is the magnetic pressure in anode spot center on pool surface. Results of calculations by this formula are given in the Table.

It follows from the data given in the Table, that velocity of melt movement towards weld pool bottom part essentially depends on anode current density and weld pool dimensions, i.e. flow velocities grow with reduction of the radius of current-conducting channel on the anode and the greater, the larger the pool volume.

The above estimates are very approximate, i.e. they are based on unidimensional consideration of liquid metal movement (Bernoulli equation, hydraulic approximation). More accurate calculations should take into account the fact that magnetic pres-

Velocities of melt flows, at which velocity head balances magnetic pressure in the weld pool

R_e , mm	R_v , mm	$P_{mag}^{(0)}$, Pa	V , cm/s	$F_{mag,z}^{(0)}$, N/m ³
1	1	292	27	$1.09 \cdot 10^6$
1	1.5	369	31	$1.26 \cdot 10^6$
1	2	400	32	$1.31 \cdot 10^6$
2	1	32	9	$7.0 \cdot 10^4$
2	1.5	55	12	$1.15 \cdot 10^5$
2	2	74	14	$1.45 \cdot 10^5$
3	1	7	4	$1.11 \cdot 10^4$
3	1.5	14	6	$2.11 \cdot 10^4$
3	2	21	7	$3.09 \cdot 10^4$

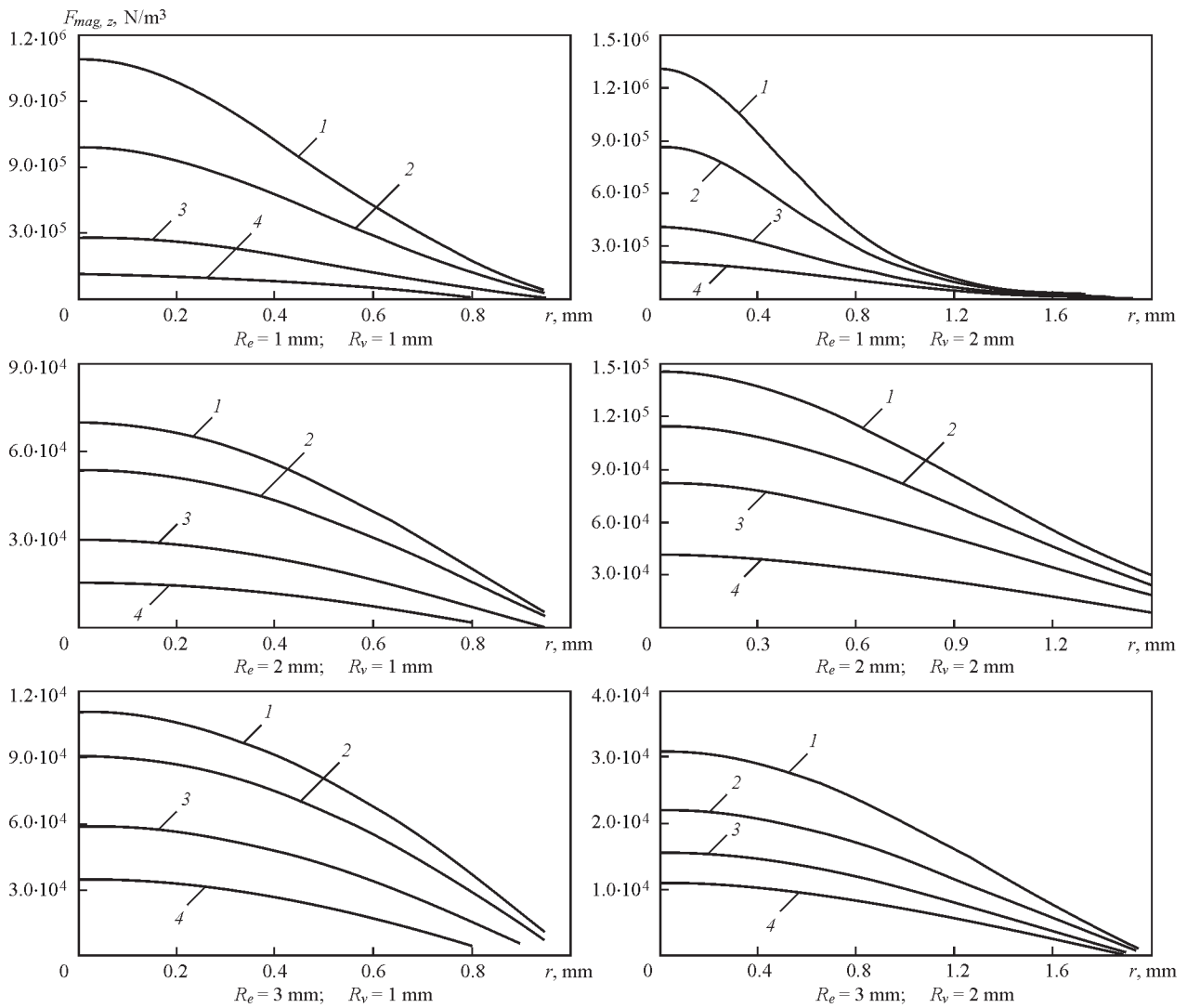


Figure 11. Distribution of F_{mag} in the weld pool: 1 — $z=0$; 2 — 0.1; 3 — 0.3; 4 — 0.5 mm

sure gradient creates a complexly distributed bulk force $\vec{F}_{mag} = \{F_{mag,r}, F_{mag,z}\}$ in the melt. In keeping with the first of equations (9), $F_{mag,r}$ component is equal to $-\frac{H_{\theta}^2}{r}$, and $F_{mag,z}$ component is presented as $F_{mag,z} = \frac{\partial P_{mag}}{\partial z}$.

Let us consider the influence of weld pool and current channel dimensions on the magnitude of axial component of force $F_{mag,z}$ (Figure 11). Similar to magnetic pressure (see Figure 10), axial component of magnetic force \vec{F}_{mag} is maximal in anode spot center and rises with increase of current density on anode surface, as well as with increase of molten metal volume (see the last column in the Table). This component of the force has a quite considerable magnitude: at $R_e = 3$ mm it is comparable with bulk density of gravitational force ($F_{grav} = 7.64$ N/m³), applied to the metal, and at $R_e = 1$ mm it exceeds the gravitational force by more than an order of magnitude. $F_{mag,z}$ component decreases rapidly as the function of radius, so that its magnitude at $r > 1$ mm is negligibly small compared

to axial values. Contrarily, radial component $F_{mag,r}$, rises monotonically at increase of radius and reaches its maximum value (comparable with $F_{mag,r}$ by order of magnitude) at $r \approx 1$ mm. Thus, magnetic force F_{mag} , being predominantly axial by its direction, has a centripetal component, which, unlike consideration of the hydrodynamic process in Bernoulli approximation, is capable of increasing the velocity of molten metal flow towards the weld pool bottom part.

In conclusion, one can say that arc plasma interaction with the metal being welded in nonconsumable electrode welding is realized through the arc anode region that determines (see, for instance [9, 10]) such, important in terms of weld formation, characteristics as density of heat flow into the anode and density of anode electric current. Heat flow density distribution in the anode is responsible for heat conductivity mechanism of energy transfer in the metal being welded. It was from exactly such positions that N.N. Rykalin constructed [11] the theory of thermal processes in welding, not taking into account the con-

vective mechanism of heat transfer in the weld pool. Contrarily, the law of current density distribution in the anode, which determines the force impact of arc current on the molten metal, is responsible for the magnitude and direction of hydrodynamic flows in the melt, and, therefore, also for convective heat transfer in the weld pool. To increase the penetrability of the arc with refractory cathode, it is important to organize sufficiently intensive melt flows, directed from overheated near-anode zone of weld pool surface to its bottom part. As shown above, such a nature of liquid metal flow is provided by compressive action of vortex component of Lorentz force. Size of current-conducting channel on anode surface also has an essential influence on magnitude of magnetic force and velocity of downward flow of the melt: the higher the electric current contraction on the anode, the greater the magnitude of axial component of magnetic force, and the higher the speed of melt movement (see Table). This leads to a conclusion, important in terms of practical applications: to increase the arc penetrability in nonconsumable electrode welding, it is necessary to find technological means to reduce the size of current-conducting channel, and to increase anode current density, respectively.

In fundamental terms, the size of anode spot and distribution of current density in it are determined by a combination of factors, related to arcing conditions and thermal state of melt surface: welding current, arc length, plasma gas composition, temperatures of near-anode plasma and melt free surface, distribution of anode potential drop along weld pool surface. At present, welding science has a number of technological measures in its arsenal, which allows regulation (reduction) of the size of current-conducting channel of the arc in the anode. One of such methods is A-TIG welding process based on application of activating fluxes (see, for instance, [12]). Let us give for comparison macrosections of welds (Figure 12, provided by D.V. Kovalenko) in TIG and A-TIG welding in argon of 6 mm stainless steel plate.

As follows from this Figure, at the same values of arc power and length, and welding speed, penetration depth is two higher greater in A-TIG welding, than in TIG welding. This technological result is due to significantly smaller dimensions of the anode spot in A-TIG welding, compared to TIG process (current-conducting channel radius is approximately equal to 2.5 mm and 6 mm, respectively).

We will also point out other possibilities of increasing electric current density in the region of anode attachment of the arc with refractory cathode. In hybrid welding (TIG + CO₂ laser), as shown in Reference

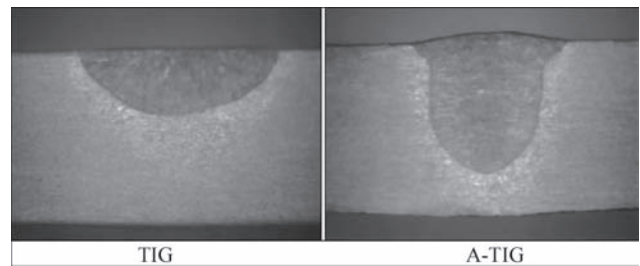


Figure 12. Weld shapes at the same arc power $P = 1400$ W; arc length $l = 1.5$ mm and welding speed $V = 100$ mm/min

[13], the nature of distribution of anode potential drop along weld pool surface changes, due to additional heating of near-anode plasma by laser radiation. This generates the radial component of current density in near-anode plasma, and leads to increase of current density in near-axial portions of the arc anode region.

Application of other shielding gases or their mixtures (He; Ar + H₂) instead of Ar, also leads to reduction of the size of current channel in the arc column, and of the cross-sectional size of the region of anode attachment of the arc, respectively. There is ground to believe [14] that the size of anode current channel decreases, compared to direct current welding, also in welding with high-frequency modulated current. Penetration depth becomes greater at application of the above-listed technological means. Physical mechanisms that cause the effect of anode current contraction are different in all the considered cases, however, the result — increase of arc penetrability by descending melt flows — is the same.

It should be mentioned here that the force impact of welding current on weld pool metal is not the only cause for excitation of hydrodynamic processes running in the pool. Note that the half-width of the weld in TIG welding (Figure 12) noticeably exceeds the penetration depth. The possible causes for such a weld shape can be direct thermocapillary Marangoni convection and viscous friction of arc plasma against the molten metal surface, which form melt flow directed along the pool free surface, which transports overheated metal from the center to pool side surface. The arising subsurface vortex transfers «cold» metal from the melting front to pool center in its reverse flow, reducing the conductive component of heat flow to pool bottom part.

Analysis of the influence of force factors on weld pool hydrodynamics given in this paper, and performed numerical estimates lead to the conclusion that valid calculated prediction of weld pool shape and thermal cycles in welded joint HAZ can be achieved only when convective flow of energy in the weld pool is adequately allowed for. Contrarily, the models based on heat conductivity mechanism of en-

ergy transfer, may lead to quite distorted views about the above-mentioned parameters.

1. Hsu, K.C., Etemadi, K., Pfender, E. (1983) Study of the free-burning high-intensity argon arc. *J. of Appl. Phys.*, **54**(3), 1293–1301.
2. Hsu, K.C., Pfender, E. (1983) Two-temperature modeling of the free-burning high-intensity arc. *Ibid.*, **54**(8), 4359–4366.
3. Fan, H.G., Kovacevic, R. (2004) A unified model of transport phenomena in gas metal arc welding including electrode, arc plasma and molten pool. *J. Phys. D: Appl. Phys.*, **37**, 2531, 2544.
4. Nishiyama, H. et al. (2006) Computational simulation of arc melting process with complex interactions. *ISIJ Int.*, **46**(5), 705–711.
5. Hu, J., Tsai, H.L. (2007) Heat and mass transfer in gas metal arc. Pt 1: The arc. *Int. J. Heat and Mass Transfer*, **50**, 833–846.
6. Hu, J., Tsai, H.L. (2007) Heat and mass transfer in gas metal arc. Pt 2: The metal. *Ibid.*, **50**, 808–820.
7. Murphy Anthony, B. (2011) A self-consistent three-dimensional model of the arc, electrode and weld pool in gas-metal arc welding. *J. Phys. D: Appl. Phys.*, **44**, 194009.
8. Mougénot, J. et al. (2013) Plasma-weld pool interaction in tungsten inert-gas configuration. *Ibid.*, **46**, 135206.
9. Krikent, I.V., Krivtsun, I.V., Demchenko, V.F. (2012) Modelling of processes of heat-, mass- and electric transfer in column and anode region of arc with refractory cathode. *The Paton Welding J.*, **3**, 2–6.
10. Krivtsun, I.V., Demchenko, V.F., Krikent, I.V. (2010) Model of the processes of heat-, mass- and charge transfer in the anode region and column of the welding arc with refractory cathode. *Ibid.*, **6**, 2–9.
11. Rykalin, N.N. (1951) *Calculations of thermal processes in welding*. Moscow: Mashgiz.
12. Yushchenko, K.A., Kovalenko, D.V., Kovalenko, I.V. (2001) Application of activators for TIG welding of steels and alloys. *The Paton Welding J.*, **7**, 37–43.
13. Krivtsun, I.V., Krikent, I.V., Demchenko, V.F. et al. (2015) Interaction of CO₂-laser radiation beam with electric arc plasma in hybrid (laser + TIG) welding. *Ibid.*, **3/4**, 6–15.
14. Zhao, J., Sun, D., Hu, S. (1992) Anode behavior of high frequency pulse TIG welding arc. *Transact. China Weld. Inst.*, **13**(1), 59–66.

Received 14.02.2017